Kinetic Simulation of Effects of Secondary Electron Emission on Electron Temperature in Hall Thrusters

IEPC-2005-078

D. Sydorenko[*] and A. Smolyakov[†]

University of Saskatchewan, Saskatoon, SK, S7H3E6, Canada

I. Kaganovich[‡] and Y. Raitses[§]

Princeton University, Princeton, NJ, 08543, USA

The particle-in-cell code has been developed for kinetic simulations of Hall thrusters with a focus on plasma-wall interaction. The secondary electron emission effect on power losses in a thruster discharge is shown to be quite different from what was predicted by previous fluid and kinetic studies. In simulations, the electron velocity distribution function is strongly anisotropic, depleted at high energy and non-monotonic. Secondary electrons form two beams propagating between the walls of a thruster channel in opposite radial directions. The beams of secondary electrons produce secondary electron emission themselves, depending on their energy at the moment of impact with the wall, which is defined by the local axial accelerating electric field in the thruster as well as by the electron transit time between the walls. Under such conditions, the sheaths at the plasma-wall interfaces can become space charge saturated if the emission produced by the secondary electron beams is strong. The contribution of the beams to the particles and energy wall losses may be much larger than that of the plasma bulk electrons. The average energy of plasma bulk electrons is far less important for the space charge saturation of the sheath than it is in plasmas with a Maxwellian electron velocity distribution function. Recent experimental studies may indirectly support the results of these simulation, in particular, with respect to the electron temperature saturation and the channel width effect on the thruster discharge.

[*]Graduate student, Department of Physics and Engineering Physics, dms169@mail.usask.ca.
[†]Professor, Department of Physics and Engineering Physics, andrei.smolyakov@usask.ca.
[‡]Research physicist, Princeton Plasma Physics Laboratory, ikaganov@pppl.gov.
[§]Research physicist, Princeton Plasma Physics Laboratory, yraitses@pppl.gov.

Nomenclature

x	= coordinate normal to the walls
t	= time
$v_{x,y,z}$	= velocity components of an electron
w	= kinetic energy of an electron
$w_{x,y,z}$	= kinetic energy of electron motion in $\{x, y, z\}$ direction respectively
m	= electron mass
M	= ion mass
e	= elementary charge
L	= width of the plasma slab
$E_{x,z}$	= components of the electric field intensity (subscript z for the applied and x for the self-consistent field)
B_x	= induction of the applied magnetic field
Φ	= electrostatic potential relative to the dielectric wall at $x = L$
n_a	= neutral gas density
n_e	= electron density
ν_{turb}	= frequency of "turbulent" collisions
ν_{en}	= frequency of electron-neutral collisions
ν_{eff}	= effective frequency of collisions
λ_c	= electron mean free path between two collisions
μ_c	= collisional electron mobility across the magnetic field
r_L	= electron Larmor radius
ω_c	= electron cyclotron frequency
Δw_{par}	= contribution of the axial electric field to the energy of electron motion parallel to the walls after a single "turbulent" or electron-neutral collision
Γ_1	= total primary electron flux towards one wall
Γ_2	= total secondary electron flux emitted by one wall
γ	= total secondary electron emission coefficient
γ_{cr}	= threshold value of the total secondary electron emission coefficient, which makes the emission space charge limited
T_{cr}	= critical electron temperature, the threshold for a plasma with a Maxwellian velocity distribution, which causes the space charge limited secondary electron emission
γ_b	= partial emission coefficient of a secondary electron beam
γ_p	= partial emission coefficient of plasma electrons
w_b	= average energy of a secondary electron beam when it impinges on the wall
w_p	= average energy of plasma electrons when they impinge on the wall
Γ_b	= primary electron flux towards one wall due to the electrons emitted from the opposite wall
Γ_p	= primary electron flux towards one wall due to the electrons from the plasma bulk
α	= coefficient of penetration of the beam of secondary electrons through the plasma
$u_{y,z}$	= components of flow velocity of a secondary electron beam in y and z directions respectively
J_z	= electric current density along z axis in simulations
J_{exp}	= experimental value of the electric current density along the thruster axis due to electrons only

I.   Introduction

SECONDARY electron emission (SEE) at the plasma-wall interface decreases the plasma potential relative to the wall and thus increases the flux of electrons from plasma to the wall.[1] The intensity of SEE is characterized by the emission coefficient $\gamma = \Gamma_2/\Gamma_1$, where Γ_1 and Γ_2 are correspondingly the primary and the secondary electron fluxes. Typically the emission coefficient increases when the electron temperature increases. If the emission coefficient exceeds the critical value $\gamma_{cr} \simeq 1 - 8.3(m/M)^{1/2}$, where m and M are the electron and ion mass respectively, the SEE turns to the space charge limited (SCL) regime, when part of the emitted electron current is reflected by the negative potential drop adjacent to the wall. The lowest electron temperature of a plasma with a Maxwellian electron velocity distribution function (EVDF), which causes SCL SEE, is called the critical electron temperature T_{cr}.[2] Transition to the SCL regime is accompanied by the considerable growth of the primary electron flux and is an important factor limiting the electron temperature.

Operation of a Hall thruster is strongly affected by SEE from thruster channel walls. The fluid theories[2−5] predict fast electron cooling due to wall losses and saturation of the electron temperature with the growth of the discharge voltage. In fact, the saturation of the electron temperature with the discharge voltage (Joule heating) was recently measured in a 2 kW Hall thruster.[6] However, in experiments[6,7] the electron temperature inside the thruster channel was several times higher than T_{cr}, which is the maximum value for the electron temperature predicted in Ref. 2. The fluid theories assume that the EVDF is Maxwellian. Kinetic studies of plasmas in Hall thrusters[8,9] reveal the depletion of the high energy tail of EVDF and the reduction of the electron losses to the wall compared with fluid theories. It was shown in Ref. 10 for electron cyclotron resonance discharges that the EVDF near a wall is far away from a Maxwellian EVDF and is strongly anisotropic. Therefore, the proper analysis of the plasma-wall interaction requires kinetic plasma simulations.

The complete three-dimensional kinetic simulation of plasma discharges consumes a tremendous amount of computer time. However, in the accelerating region of a Hall thruster the radial magnetic field is strong and the EVDF is established on a spatial scale much smaller than the entire length of the accelerating region. Therefore, to obtain the EVFD it is sufficient to consider a thin radial section of the accelerating region, which may be approximated by a one-dimensional model. A particle-in-cell (PIC) code has been developed for simulations of a plasma layer immersed in external electric and magnetic fields and bounded by dielectric walls. The PIC code self-consistently resolves in one spatial dimension both the sheath and the plasma bulk regions. The parallel execution of the PIC code on multiple processors allows to simulate the evolution of the plasma slab with width of hundreds of Debye lengths over the time intervals of the order of several ion transit times. The numerical study of this model reveal a number of kinetic effects, which are important for the physics of Hall thrusters. This paper describes some of the most interesting results, such as the strong anisotropy of the EVDF with beams of secondary electrons, while the detailed description can be found in our previous works[11,12] and recent papers. [12−13]

II.   Description of the model

Consider the plasma bounded by two infinite parallel dielectric walls capable to produce SEE, see Fig. 1. Axis x is directed normal to the walls. The system is uniform along axes y and z. The plasma is immersed in the external constant uniform magnetic field B_x and electric field E_z. The described system is simulated with the parallel electrostatic particle-in-cell code, which is developed on the basis of the direct implicit algorithm.[14,15] The code resolves one spatial coordinate x and three velocity components v_x, v_y, and v_z for each particle.[11,12]

Elastic, excitation and ionization collisions between electrons and neutral xenon atoms are implemented making use of the Monte Carlo model of collisions.[16] The neutral gas density is uniform across the plasma and is not changed during simulations. To account for the anomalously high electron mobility across the magnetic field in Hall thrusters, the additional "turbulent" collisions are introduced,[3] which randomly scatter particles in y-z plane without changing their energy.[17] Coulomb and ion-neutral collisions are neglected.[18]

The SEE model is similar to that of Ref. 19. The total flux of secondary electrons consists of the elastically reflected primary electrons, the inelastically backscattered primary electrons, and the true secondary electrons. Injection of these components is determined by the corresponding emission coefficients, which are functions of the energy of primary electrons and the angle of incidence.[4,19−21] The ions are neutralized after
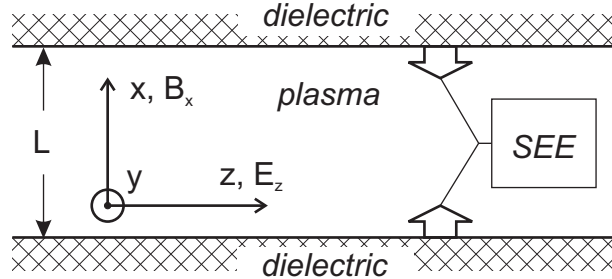
Figure 1. Schematic diagram of the simulated plasma system. The two dielectric walls represent the coaxial ceramic channel of a Hall thruster.

collision with the wall increasing the surface charge. The total emission coefficient γ agrees with the available experimental data for boron nitride ceramics grade HP.[22] It is found in simulations of xenon plasmas with a Maxwellian EVDF that for the implemented SEE model the critical electron temperature is about $T_{cr} = 19 \ eV$. For comparison, in Ref. 23 the same experimental emission coefficient data were averaged analytically over a Maxwellian EVDF and the value $T_{cr} = 18.26 \ eV$ was obtained.

The PIC code was benchmarked against the available numerical and theoretical results. The code reproduces the main results of the early sheath simulations[24] with a Maxwellian plasma source and SEE with the constant emission coefficient (for such simulations the wall at $x = 0$ is substituted by the plasma source). The linear increments of the two stream instability of a cold beam in a dense cold plasma[25] and the nonlinear saturation of the beam-plasma instability[26] are reproduced with periodic boundary conditions.

Simulations with two dielectric walls were carried out with parameters corresponding to the values experimentally measured in the $2kW$ Hall thruster for discharge voltages from 200 to 350 V.[6] The axial electric field E_z and the radial magnetic field B_x were taken at the point with maximal electron temperature, which is inside the thruster channel for the considered discharge voltage range. The neutral gas density n_a determined the frequency of electron-neutral collisions ν_{en}. The "turbulent" collision frequency ν_{turb} was adjusted such that the electron mobility μ_c due to both "turbulent" and electron-neutral collisions corresponds to the experimental value of the electron electric current density J_{exp}:

$$J_{exp} = en_e\mu_c E_z = en_e \frac{e}{m\nu_{eff}(1 + \omega_c^2/\nu_{eff}^2)} E_z \ ,$$

where $\nu_{eff} = \nu_{turb} + \nu_{en}$ is the effective frequency of collisions, ω_c is the electron cyclotron frequency.

In the next section the major results are highlighted, presenting for illustrations the data obtained in simulation with $L = 2.5 \ cm$, $E_z = 200 \ V/cm$, $B_x = 100 \ Gauss$, $n_a = 2 \cdot 10^{12} \ cm^{-3}$, $\nu_{turb} = 1.46 \cdot 10^6 \ s^{-1}$. In this simulation the plasma density averaged over the width of the plasma slab is $n_e = 3.2 \cdot 10^{11} \ cm^{-3}$ (after $6.9 \ \mu s$ of the system evolution).

III.   Results

The simulations reveal that in thruster plasmas the EVDF is anisotropic and far from Maxwellian (see Fig. 2).[11−13] The average energy of electron motion in the directions parallel to the walls $\langle w_{y,z} \rangle = \langle mv_{y,z}^2/2 \rangle$ is several times larger than the average energy of electron motion in the direction perpendicular to the walls $\langle w_x \rangle$, averaging $\langle ... \rangle$ is done over all electrons. The EVDF presented in Fig. 2 has $\langle w_x \rangle \simeq 5.7 \ eV$ and $\langle w_z \rangle \simeq 24.5 \ eV$.

Qualitatively, the anisotropy of the EVDF can be explained as follows.[12,13] The electrons gain their energy from the accelerating electric field E_z as a result of "turbulent" collisions and collisions with neutral atoms. The heating occurs in the direction parallel to the walls while the electron-neutral collisions make the electron distribution function isotropic. If the frequency of the "turbulent" collisions is much higher than the frequency of collisions with atoms $\nu_{tu} \gg \nu_{en}$, which is typical for the low voltage regimes of the thruster's operation,[6] the electrons are heated in the direction parallel to the walls much faster then the rate at which the distribution function is made isotropic resulting in the anisotropic distribution [10,27]. For high
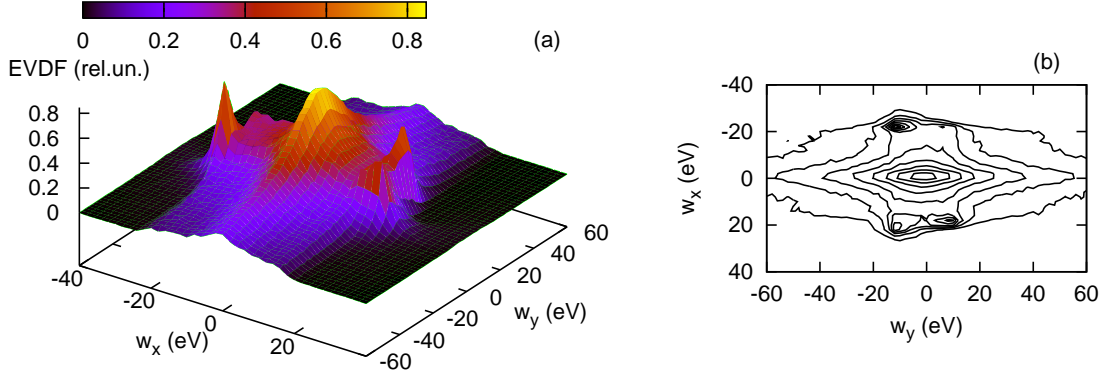
Figure 2. The electron velocity distribution over v_x and v_z in the middle of the plasma $10\ mm < x < 15\ mm$ plotted in energy coordinates (the sign marks the velocity direction). Figure (a) – 3D-plot, figure (b) – the corresponding 2D-plot with contour lines. Any two neighbor level lines in figure (b) have level difference of 0.1.

discharge voltages, the difference between the classical and the anomalous axial electron mobility decreases[6] so that $\nu_{tu} \sim \nu_{en}$. In these regimes, the anisotropy develops when the axial electric field E_z satisfies the criterion $eE_z r_L > e\Phi$. In the latter case, the electron receives a significant energy in the direction parallel to the walls $\Delta w_{par} > e\Phi$, and such electrons are easily lost to the walls as a result of the next few collision events. If the above mentioned criterion for the electric field is satisfied, one obtains $\langle w_{y,z} \rangle \sim eE_z r_L > e\Phi$ (compare lines 1 and 3 in the middle region in Fig. 3). The consistency between the plasma potential and the plasma temperature requires $\langle w_x \rangle < e\Phi$ (compare lines 2 and 3 in the middle region in Fig. 3) so that the EVDF becomes anisotropic with $\langle w_x \rangle < \langle w_{y,z} \rangle$.

Although the SEE decreases the drop of potential across the sheath, the potential of the isotropic maxwellian plasmas is of the order of several electron temperatures. However, simulations of thruster plasmas show that due to the anisotropy the plasma potential is low compared to the total average electron energy $\langle w \rangle$ and typically has the value of about tens of Volts (see line 3 in Fig. 3). Also, in the present simulations the electric field and the dynamics of plasma particles are calculated self-consistently across the whole plasma slab. As a result, the source sheaths, which are inherent in simulations with plasma sources and represent the distinct potential drops near the plasma source,[24,28] do not appear and the potential profile is smooth (line 3 in Fig. 3).
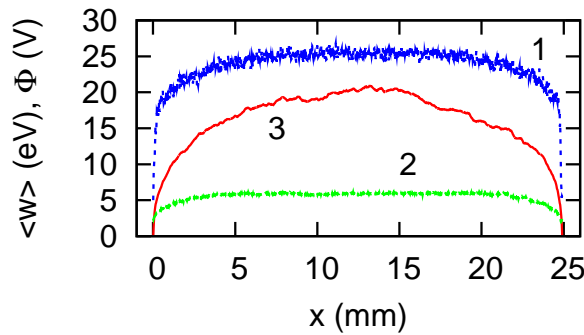

Figure 3. Spatial profiles of the average electron energy of motion in z-direction (line 1) and in x-direction (line 2), and of the electrostatic potential (line 3). The walls are at $x = 0$ and $x = 25\ mm$. Note that everywhere $\langle w_x \rangle < e\Phi < \langle w_z \rangle$

For the neutral density used in simulations the average frequency of electron-neutral collisions is $\nu_{en} \simeq 1.4 \cdot 10^6\ s^{-1}$, the average electron energy for the case presented in this section is $\langle w \rangle = 66\ eV$, the corresponding velocity is $v = 4.8 \cdot 10^6\ m/s$, and the mean free path between the two collisions with neutral atoms

(which may scatter an electron towards the wall) is $\lambda_c = v/(\nu_{en} + \nu_{tu}) = 3.4 \ m \gg L$. The mean free path is much larger than the width of the plasma slab, that is why the EVDF is strongly depleted for the energies w_x above the plasma potential $w_x > e\Phi(x)$.[10] This group of electrons forms the loss cone and is populated by electrons emitted from the walls, as well as by the electrons from the plasma bulk, which collided with neutral atoms.[11-13]

The emitted electrons move along the spiral-like trajectories: the acceleration and deceleration in x direction is combined with the cyclotron rotation in y-z plane and $E_z \times B_x$ drift in y direction (see Fig. 4a). The near-wall conductivity theory relies on such motion explaining the increase of the electron mobility across the magnetic field.[29] In the simulation presented here the 200% increase of the axial electron mobility due to the near-wall conductivity effect compared to the mobility determined by collisions with neutral atoms and "turbulent" collisions is observed.[11-13] When the near-wall conductivity effect is significant, the profile of the axial electron current density $J_z(x)$ becomes modulated, as it is predicted in Ref. 29 (see Fig. 5).
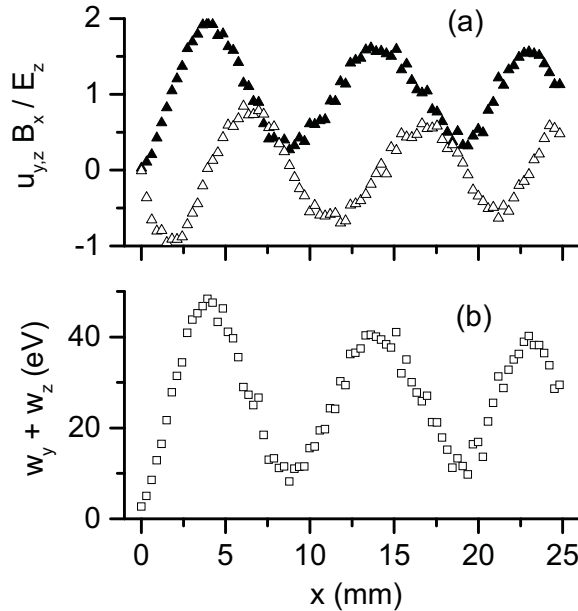

Figure 4. For the electron beam emitted from the wall $x = 0$: figure (a) represents the local flow velocities u_y (black triangles) and u_z (open triangles) versus x coordinate, figure (b) represents the local average energy $w_y + w_z$ versus x coordinate. The walls are at $x = 0$ and $x = 25 \ mm$.

Note that not only the velocity, but also the energy of motion of emitted electron parallel to the walls oscillates along the electron trajectory (see Fig. 4b). At the time of collision with the wall the average energy of beam electrons w_b exceeds the initial average energy of emission by the value of the order of $m(E_z/B_x)^2$ due to the drift motion. Therefore, in large electric field the emitted electrons may produce intense secondary electron emission themselves.[11-13] From Fig. 4b follows that w_b depends on the phase of cyclotron rotation of electrons at the moment of their impact with the wall. This phase depends on the time of transit of the emitted electrons between the walls and is defined by the distance between the walls and by the potential profile. Recently the strong effect of the channel width on thruster operation has been observed,[30] which may be related with the dependence of the energy of the secondary electron beams on the width of the channel.

The plasma bulk electrons and the beam electrons are characterized by different average energies $w_{p,b}$ at the moment of impact with the wall, and thus produce SEE with independent partial emission coefficients $\gamma_{p,b}$. Here, index p corresponds to the plasma bulk and index b – to the beam electrons. In the stationary sheath with monotonic potential profile the ratio of the particles fluxes $\Gamma_{p,b}$ of two groups of electrons is defined by the partial emission coefficients and by the coefficient of penetration of the electron beam through the plasma slab α:[12-13]

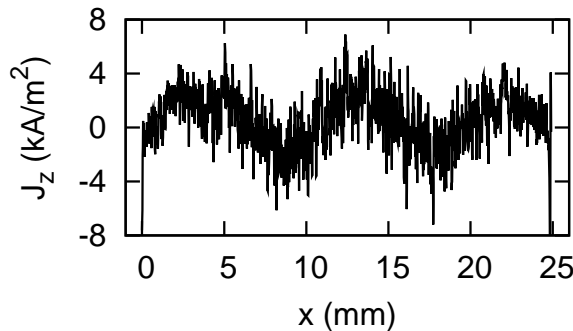$$\frac{\Gamma_b}{\Gamma_p} = \frac{\alpha\gamma_p}{1 - \alpha\gamma_b} \ , \tag{1}$$

Figure 5. Modification of the profile of the electron current density in z-direction in the regime when the near-wall conductivity is significant. The walls are at $x = 0$ and at $x = 25\ mm$.

where $\alpha = \Gamma_b / \Gamma_2 < 1$.

Equation (1) is valid if $\alpha \gamma_b < 1$ — otherwise the stationary stage is not possible. From (1) follows that if $\alpha \gamma_p \gg 1 - \alpha \gamma_b$ then $F_b \gg F_p$ and most of the electron flux to the wall is created by the secondary electron beams.

The expression for the total emission coefficient is[12−13]

$$\gamma = \frac{\gamma_p}{1 + \alpha(\gamma_p - \gamma_b)} \ . \tag{2}$$

The exact values of fluxes and emission coefficients in simulations satisfy these analytical relations. For the simulation presented in this section $w_p = 54 \pm 4\ eV$, $w_b = 35.5 \pm 0.5\ eV$ $\gamma_p = 1.02 \pm 0.06$, $\gamma_b = 0.963 \pm 0.012$, $\Gamma_p = (2.67 \pm 0.19) \cdot 10^{17}\ s^{-1} cm^{-2}$, $\Gamma_b = (1.81 \pm 0.16) \cdot 10^{18}\ s^{-1} cm^{-2}$, $\alpha = 0.911 \pm 0.024$. The fluxes measured directly in the simulation give $\Gamma_b / \Gamma_p = 6.8 \pm 1.1$, while Eq. 1 gives close value $\Gamma_b / \Gamma_p = 7.6$. The total emission coefficient measured in the simulation $\gamma = 0.97$ is the same as the value that follows from Eq. 2. Note that $\gamma < \gamma_{cr} = 0.983$ although $\gamma_p > \gamma_{cr}$.

The simulations show that the two-stream instability[31] is usually weak and does not lead to significant loss of the beam current, which results in $\alpha \simeq 1$.[12,13]

Recently in Ref. 32 the problem of the sheath formation in a bounded plasma slab in presence of the counter-propagating secondary electron beams has been considered in the fluid framework. The important effect of secondary electron emission produced by the beams of secondary electrons was not considered, thus the criterion for the SCL SEE regime obtained in Ref. 32 is valid only for low accelerating fields. The results of Ref. 32 may be obtained as the particular case of more general equation (2).

The complete kinetic study of the bounded plasma slab reveal another interesting effect. Numerous simulations have been carried out with different sets of parameters in which the "classical" stationary SCL SEE regime was not observed.[11−13] Instead, under certain conditions the structure of the sheath corresponds to the non-SCL SEE regime most of the time and quasi-periodically turns into the SCL regime for a short periods of time. During these periods the emission coefficient exceeds the SCL SEE threshold (see Fig. 6a) and the primary electron flux to the wall abruptly increases (see Fig. 6b). The sheath oscillations are described in Refs. 11-13.

IV. Conclusion

The considered model reveals several features of plasma-wall interaction in Hall thrusters, which are missed by fluid theories as well as by kinetic simulations of near wall regions carried out with the assumption that the bulk plasma has a Maxwellian EVDF. It is found that the thruster plasma is anisotropic, the secondary electrons almost freely propagate between the walls and produce secondary emission themselves. The criterion of the space charge limited secondary electron emission is modified: the average energy of electrons confined by the plasma potential may be large, while the secondary electron emission remains in the non space charge limited regime. The quasi-periodic nonlinear oscillations of the simulated plasma are observed instead of the stationary space charge limited regime of secondary electron emission. There are several practical implications of these studies: (i) the strong SEE effect on power losses and near-wall
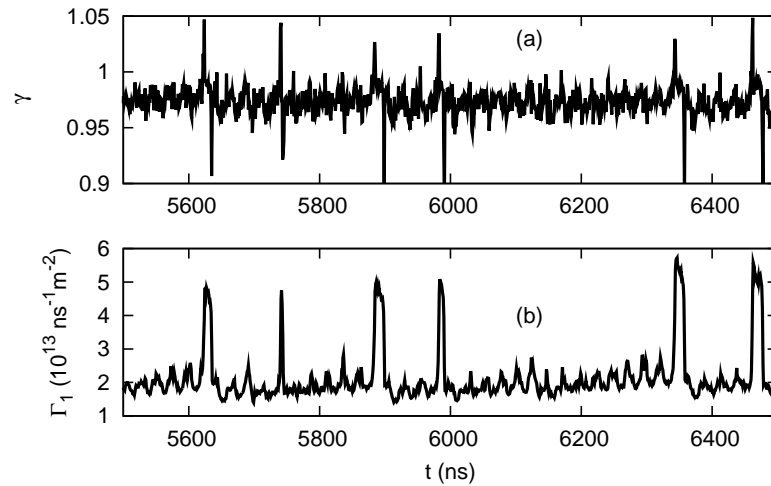
Figure 6. At the wall $x = L$**: figure (a) – the emission coefficient versus time, and figure (b) – the total primary electron flux versus time.**

conductivity in the thruster discharge is expected to occur only when the axial electric field provides the emitted electrons with sufficient additional energy; (ii) the SEE effect depends on the channel width because the energy of secondary electron beams at the moment of their impact with the walls depends on the time of electron transit between the walls. These predictions appear to be in an agreement with experimental studies.

Acknowledgments

References

[1]Hobbs, G. D. and Wesson, J. A., "Heat Flow through a Langmuir Sheath in the Presence of Electron Emission," *Plasma Physics*, Vol. 9, 1967, pp. 85, 87.

[2]Choueiri, E. Y., "Fundamental Difference Between the Two Hall Thruster Variants," *Physics of Plasmas*, Vol. 8, No. 11, 2001, pp. 5025, 5033.

[3]Keidar, M., Boyd, I. D., and Beilis, I. I., "Plasma Flow and Plasma-Wall Transition in hall Thruster channel," *Physics of Plasmas*, Vol. 8, No. 12, 2001, pp. 5315, 5322.

[4]Ahedo, E., Gallardo, J. M., and Martínez-Sánchez, M., "Effects of the Radial Plasma-Wall Interaction on the Hall Thruster Discharge," *Physics of Plasmas*, Vol. 10, No. 8, 2003, pp. 3397, 3409.

[5]Barral, S., Makowski, K., Peradzyński, Z., Gaskon, N., and Dudeck, M., "Wall Material Effects in Stationary Plasma Thrusters. II. Near-Wall and In-Wall Conductivity," *Physics of Plasmas*, Vol. 10, No. 10, 2003, pp. 4137, 4152.

[6]Raitses, Y., Staack, D., Smirnov, A., and Fisch N. J., "Space Charge Saturated Sheath Regime and Electron Temperature Saturation in Hall Thrusters," *Physics of Plasmas*, Vol. 12, No. 7, 2005, 073507, 10 p.

[7]Staack, D., Raitses, Y., and Fisch, N. J., "Temperature Gradient in Hall Thrusters," *Applied Physics Letters*, Vol. 84, No. 16, 2004, pp. 3028, 3030.

[8]Meezan, N. B. and Cappelli, M. A., "Kinetic Study of Wall Collisions in a Coaxial Hall Discharge," *Physical Review E*, Vol. 66, No. 3, 2002, 036401, 10 p.

[9]Batishchev, O. and Martínez-Sánchez, M., *28th International Electric Propulsion Conference*, Toulouse, France, 2003, Electric Rocket Propulsion Society, Cleveland, OH, 2003d, IEPC paper 2003-188.

[10]Kaganovich, I., Mišina, M., Berezhnoi, S. V., and Gijbels, R., "Electron Boltzmann Kinetic Equation

Averaged over Fast Electron Bouncing and Pitch-Angle Scattering for Fast Modeling of Electron Cyclotron Resonance Discharge," *Physical Review E*, Vol. 61, No. 2, 2000, pp. 1875, 1889.

[11]Sydorenko, D. Y. and Smolyakov, A. I., "Simulation of Secondary Electron Emission Effects in a Plasma Slab in Crossed Electric and Magnetic Fields," *APS DPP 46th Annual Meeting*, Savannah, GA, November 15-19, 2004, NM2B.008.

[12]Sydorenko, D., Smolyakov, A., Kaganovich, I., and Raitses, Y., "Modification of Electron Velocity Distribution in Bounded Plasmas by Secondary Electron Emission," *Workshop "Nonlocal Collisionless Phenomena in Plasmas,"* Princeton Plasma Physics Laboratory, Princeton, NJ, August 2-4, 2005; to be submitted to the IEEE Transactions on Plasma Sciences.

[13]Kaganovich, I., Raitses, Y., Sydorenko, D., and Smolyakov, "Effects of Non-Maxwellian EEDF on Particle and Heat Losses from a Plasma in Presence of Secondary Electron Emission," *PPPL preprint*, URL: http://www.pppl.gov/pub_report.

[14]Langdon, A. B., Cohen, B. I., and Friedman, A., "Direct Implicit Large Time-Step Particle Simulation of Plasmas," *Journal of Computational Physics*, Vol. 51, 1983, pp. 107, 138.

[15]Gibbons, M. R. and Hewett, D. W., "The Darwin Direct Implicit Particle-in-Cell (DADIPIC) method for Simulation of Low Frequency Plasma Phenomena," *Journal of Computational Physics*, Vol. 120, 1995, pp. 231, 247.

[16]Vahedi, V. and Surendra, M., "A Monte Carlo Collision Model for the Particle-in-Cell Method: Applications to Argon and Oxygen Discharges," *Computer Physics Communications*, Vol. 87, No, 1-2, 1995, pp. 179, 198.

[17]Smirnov, A., Raitses, Y., and Fisch, N. J., "Electron Cross-Field Transport in a Low Power Cylindrical Hall Discharge," *Physics of Plasmas*, Vol. 11, No. 11, 2004, pp. 4922, 4933.

[18]Boeuf, J. P. and Garrigues, L., "Low Frequency Oscillations in a Stationary Plasma Thruster," *Journal of Applied Physics*, Vol. 84, No. 7, 1998, pp. 3541, 3554.

[19]Gopinath, V. P., Verboncoeur, J. P., and Birdsall, C. K., "Multipactor Electron Discharge Physics Using an Improved Secondary Emission Model," *Physics of Plasmas*, Vol. 5, No. 5, 1998, pp. 1535, 1540.

[20]Seiler, H., "Secondary Electron Emission in the Scanning Electron Microscope," *Journal of Applied Physics*, Vol. 54, No. 11, 1983, pp. R1, R18.

[21]Vaughan, J. R. M., "A New Formula for Secondary Emission Yield," *IEEE Transactions on Electron Devices*, Vol. 36, No. 9, 1989, pp. 1963, 1967.

[22]Dunaevsky, A., Raitses, Y., and Fisch, N. J., "Secondary Electron Emission from Dielectric Materials of a Hall Thruster with Segmented Electrodes," *Physics of Plasmas*, Vol. 10, No. 6, 2003, pp. 2574, 2577.

[23]Smirnov, A., Raitses, Y., and Fisch, N. J., "Enhanced Ionization in the Cylindrical Hall Thruster," *Journal of Applied Physics*, Vol. 94, No. 2, 2003, pp. 852, 857.

[24]Schwager, L. A., "Effects of Secondary and Thermionic Electron Emission on the Collector and Source Sheaths of a Finite Ion Temperature Plasma Using Kinetic Theory and Numerical Simulation," *Physics of Fluids B*, Vol. 5, No. 2, 1993, pp. 631, 645.

[25]Mikhailovskii, A. B., *Theory of plasma instabilities*, New York, Consultants Bureau, 1974, pp. 12, 14.

[26]Matsiborko, N. G., Onishchenko, I. N., Shapiro, V. D., and Shevchenko, V. I., "On Non-Linear Theory of Instability of a Mono-Energetic Electron Beam in Plasma," *Plasma Physics*, Vol. 14, 1972, pp. 591, 600.

[27]Kaganovich, I., "Modeling of Collisionless and Kinetic Effects in Thruster Plasmas," the IEPC05 paper 096.

[28]Taccogna, F., Longo, S., and Capitelli, M., "Plasma Sheaths in Hall Discharge," *Physics of Plasmas*, Vol. 12, No. 9, 2005, 093506, 14 p.

[29]Morozov, A. I. and Savel'ev, V. V., " Theory of the Near-Wall Conductivity," *Plasma Physics Reports*, Vol. 27, No. 7, 2001, pp. 570, 575.

[30]Raitses, Y., Staack, D., Keidar, M., and Fisch N. J., "Electron-Wall Interaction in Hall Thrusters," *Physics of Plasmas*, Vol. 12, No. 5, 2005, 057104, 9 p.

[31]Franklin, R. N. and Han, W. E., "The Stability of the Plasma-Sheath with Secondary Emission," *Plasma Physics and Controlled Fusion*, Vol. 30, No. 6, pp. 771, 784.

[32]Ahedo, E. and Parra, F. I., "Partial Trapping of Secondary Electron Emission in a Hall Thruster Plasma," *Physics of Plasmas*, Vol. 12, 2005, 073503, 7 p.